Inorganic Chemistry

Article

pubs.acs.org/IC

D-Penicillamine Tripodal Derivatives as Efficient Copper(I) Chelators

Anne-Solène Jullien,[†,‡] Christelle Gateau,[†,‡] Colette Lebrun,[†,‡] Isabelle Kieffer,[§,∥] Denis Testemale,[§,⊥,#] and Pascale Delangle*[,†,‡]

[†]Université Grenoble Alpes, INAC, SCIB, RICC F-38000 Grenoble, France

[‡]CEA, INAC, SCIB, Laboratoire de Reconnaissance Ionique et Chimie de Coordination, F-38054 Grenoble, France

[§]BM30B/FAME beamline, ESRF, F-38043 Grenoble cedex 9, France

[∥]Observatoire des Sciences de l'Univers de Grenoble, UMS 832 CNRS Université Joseph Fourier, F-38041 Grenoble cedex 9, France

[⊥]Université Grenoble Alpes, Institut NEEL, F-38042 Grenoble, France

[#]CNRS, Institut NEEL, F-38042 Grenoble, France

Supporting Information

ABSTRACT: New tripodal metal-chelating agents derived from nitrilotriacetic acid (NTA) and extended by three unnatural amino acids D-penicillamine (D-Pen) are presented. D-Pen is actually the drug most extensively used to treat copper (Cu) overload in Wilson's disease and as such is a very attractive building block for the design of chelating agents. D-Pen is also a bulkier analogue of cysteine, with the β-methylene hydrogen atoms replaced by larger methyl groups. The hindrance of the *gem*-dimethyl group close to the thiol functions is demonstrated to influence the speciation and stability of the metal complexes. The ligands $\mathbf{L^4}$ (ester) and $\mathbf{L^5}$ (amide) were obtained from NTA and commercial D-Pen synthons in four and five steps with overall yields of 14 and 24%, respectively. Their ability to bind Cu(I), thanks to their three thiolate functions, has been investigated using both spectroscopic and analytical methods. UV, CD, and NMR spectroscopy and mass spectrometry evidence the formation of two Cu(I) complexes with $\mathbf{L^5}$: the mononuclear complex $\mathbf{CuL^5}$ and one cluster $(Cu_2\mathbf{L^5})_2$. In contrast, the bulkier ethyl ester derivative $\mathbf{L^4}$ cannot accommodate the mononuclear complex in solution and thus forms exclusively the cluster $(Cu_2\mathbf{L^4})_2$. Cu K-edge X-ray absorption spectroscopy (XAS and EXAFS) confirms that Cu(I) is bound in trigonal-planar sulfur-only environments in all of these complexes with Cu- - -S distances ranging from 2.22 to 2.23 Å. Such C_3-symmetric CuS_3 cores are coordination modes frequently adopted in Cu(I) proteins such as metallothioneins. These two ligands bind Cu(I) tightly and selectively, which makes them promising chelators for intracellular copper detoxification in vivo.

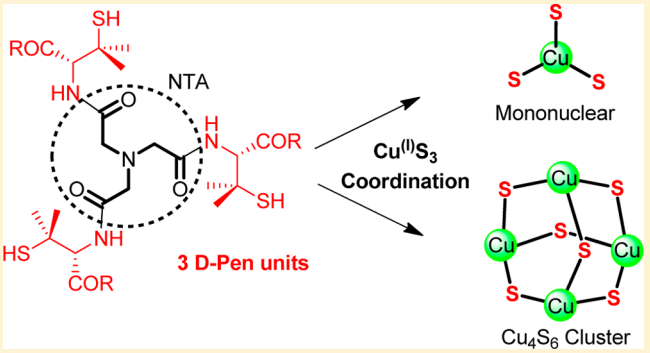

INTRODUCTION

Some metals such as copper, iron, and manganese play crucial roles in the functioning and structural integrity of proteins.[1] In metalloproteins, these metal ions carry out structural, regulatory, or catalytic roles. In particular, the copper ions play key roles in all living organisms and are used as cofactors of several enzymes involved in electron transfers, oxidase and oxygenase activities, and detoxification of oxygen radicals. However, high concentrations of copper can be deleterious, leading to oxidative damage of proteins, lipids, and nucleic acids. That is why copper concentration is rigorously controlled by subtle cellular mechanisms, the main organ of copper homeostasis being the liver.[2−5] In some cases, these regulation mechanisms can be faulty and copper accumulates at a toxic level in cells. Wilson's disease is one of the major genetic disorders of copper metabolism in humans.[6−9] In this rare disease the ATP-ase ATP7B in charge of the excretion of excess Cu from the liver cells is defective. Consequently, Cu accumulates in the liver cells, where it is involved in Fenton-like reactions, which produce toxic hydroxyl radicals. That is why chelators, such as the British anti-Lewisite (BAL), dimercaptosuccinic acid (DMSA), dimercaptopropanesulfonic acid (DMPS), triethylenetetramine (TETA), and D-penicillamine (D-Pen) have been used to treat Wilson's disease.[10,11] BAL was introduced in 1951 to treat Wilson's disease patients from neurological symptoms.[12] However, since BAL and its hydrophilic derivatives DMSA and DMPS have shown many unwanted side effects, other chelators were searched for. In particular, D-Pen was introduced in 1956[13] and is currently the most widely used treatment of Wilson's disease around the world. However, some side effects related to this therapy have been reported.[14] More precisely, it has been shown that D-Pen can contribute to increase the neurologic deterioration

Received: February 24, 2014
Published: April 25, 2014

 © 2014 American Chemical Society dx.doi.org/10.1021/ic5004319 | Inorg. Chem. 2014, 53, 5229−5239

expressed by some Wilson's disease patients, which may be due to a lack of specificity of the drug.

Our laboratory has been involved in the design of new drugs to treat Wilson's disease for several years.[15,16] These new drugs are copper chelators with the following properties: (i) they show a high affinity for Cu(I), which is the oxidation state of excess intracellular Cu, (ii) they are selective for Cu(I) with respect to potentially competing endogeneous metals such as Zn(II), and (iii) they are water-soluble. Mimics of binding sites found in proteins involved in Cu homeostasis are good candidates that meet all these expectations. A first strategy used peptide sequences of the copper binding loop of metallochaperones such as Atox1, which transfer the Cu(I) ion to ATP7B in the liver cells. These metal-binding loops contain two cysteine residues and were introduced in cyclodecapeptides, which complex digonally the Cu(I) ion with a dissociation constant on the order of 10^{-17}.[17−19] Metallothioneins are also attractive Cu(I) chelating proteins, since they are natural metal sequestering agents synthesized by cells in case of Cu overload and involved in Cu intracellular detoxification.[20−23] Interestingly, in metallothioneins Cu(I) is tightly bound in CuS_3 coordination environments provided by three thiolates of cysteine residues.[24] The stability of the Cu(I) complexes with metallothioneins is exceptionally large, with dissociation constants on the order of 10^{-19}.[25] This led us to design pseudopeptide[26] ligands with three cysteines attached with peptide bonds to C_3-symmetric nonbiological scaffolds, which act as platforms to direct the three thiolate binding arms in the same direction to coordinate the Cu(I) ion.[27,28] Nitrilotriacetic acid (NTA) was chosen as a tripodal anchor and led to the three cysteine derivatives $\mathbf{L^1}$−$\mathbf{L^3}$ depicted in Figure 1. It has been established that the carboxylic acid

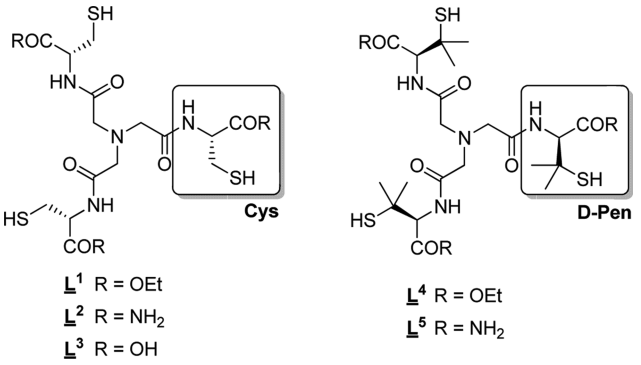

Figure 1. Structures of the Cu(I) cysteine-based chelators $H_3\mathbf{L^1}$−$H_3\mathbf{L^3}$ from previous work[27,28,41,42] and the Cu(I) D-penicillamine-based chelators $H_3\mathbf{L^4}$ and $H_3\mathbf{L^5}$ (this work).

derivative $\mathbf{L^3}$ forms mixtures of Cu(I) complexes of low affinity, whereas both $\mathbf{L^1}$ (ester) and $\mathbf{L^2}$ (amide) bind tightly the Cu(I) ion in C_3-symmetric species, either mononuclear (Cu**L**) or polymetallic ($(Cu_2\mathbf{L})_3$). In both types of complexes, Cu(I) ions are coordinated in CuS_3 environments[29] as in many Cu proteins,[30−33] in particular metallothioneins.[24,34,35] The structural analogies of Cu complexes with $\mathbf{L^1}$ or $\mathbf{L^2}$ and metallothioneins allow us to rationalize the high affinities of the pseudopeptide ligands for Cu(I), with dissociation constants of $10^{-19.2}$ ($\mathbf{L^1}$) and $10^{-18.8}$ ($\mathbf{L^2}$).[28] Moreover, these Cu(I) chelating agents inspired from either metallochaperones or metallothioneins are selective for Cu(I) with respect to the essential ion Zn(II), which is important for the detoxification of Cu(I) in vivo without altering the homeostasis of zinc.

Since these ligands are designed to chelate intracellular copper, in particular in the liver, they have to be internalized into hepatocytes. Therefore, two of these bioinspired efficient Cu(I) chelating agents have been functionalized with sugar units to target liver cells via the asialoglycoprotein receptors (ASGP-R).[16,17,36] Both glycoconjugates were demonstrated to release high-affinity Cu chelating agents in the hepatic cells. This confirms that the use of intracellular Cu(I) chelators is very promising to treat Cu overload.

The sulfur tripods $\mathbf{L^1}$ and $\mathbf{L^2}$ derived from NTA demonstrate the most promising Cu(I) chelating properties with large affinities and selectivities for Cu(I). Therefore, we are currently exploring the metal chelating properties of NTA pseudopeptides functionalized with various metal-coordinating amino acids. In particular, D-Pen is currently the drug most extensively used to treat Cu overload in Wilson's disease and, as such, represents a very attractive building block for the design of chelating agents. D-Pen is also a bulkier analogue of cysteine with the β-methylene hydrogen atoms replaced with larger methyl groups. Incidentally, its insertion in peptide sequences in place of cysteine has been demonstrated to provide more steric bulk in the coordination sphere of Cd(II)[37−39] or Co(II)[40] and to favor a MS_3 geometry.

In this paper, we present the new tripodal architectures $\mathbf{L^4}$ and $\mathbf{L^5}$ (Figure 1) derived from D-Pen. A first objective was to explore the effect of replacing the cysteine units with the more hindered D-Pen units and therefore to evidence the influence of the *gem*-dimethyl group onto the metal complexing properties in the tripodal architectures. In addition, the use of non-natural amino acids is known to disfavor hydrolysis in vivo. The ester ($\mathbf{L^4}$) and amide ($\mathbf{L^5}$) derivatives have been synthesized, and their ability to bind Cu(I) thanks to their thiolate functions has been proven using both spectroscopic and analytical methods such as UV spectroscopy (UV), circular dichroism (CD), mass spectrometry (MS), nuclear magnetic resonance (NMR), and X-ray absorption spectroscopy (XAS). The *gem*-dimethyl group close to the thiol function influences the reactivity of the D-Pen residue and also the speciation and stability of the metal complexes.

EXPERIMENTAL SECTION

Syntheses. Detailed experimental procedures for the syntheses of all intermediates and ligands $\mathbf{L^4}$ and $\mathbf{L^5}$ are given in the Supporting Information, together with their characterization data.

Samples for Physicochemical Experiments. The chelators $\mathbf{L^4}$ and $\mathbf{L^5}$ and Cu(I) are susceptible to air oxidation; therefore, the samples for physicochemical studies were all prepared in the glovebox under an argon atmosphere and sealed if used outside the glovebox. The samples were dispersed in mixtures containing different proportions of extrapure water buffered at pH 7.4 with the appropriate buffer and acetonitrile or buffered D_2O and CD_3CN for NMR experiments. At least 10% of acetonitrile was added to each sample to prevent Cu(I) dismutation.[43] Glycerol was added for X-ray absorption spectroscopy (XAS) experiments to prevent the degradation of the samples at cryogenic temperatures. In each case, the final concentration of the ligand solution was determined by measuring the D-penicillamine (D-Pen) derivative free thiol concentration following Ellman's procedure.[44] The Cu(I) solutions were prepared by dissolving the appropriate amount of $Cu(CH_3CN)_4PF_6$ in acetonitrile or CD_3CN for NMR experiments. The final concentration was determined by adding an excess of sodium bathocuproine disulfonate (BCS) and measuring the absorbance of $Cu(BCS)_2^{3-}$.[33] The Zn(II) solutions used for titrations were prepared by dispersing

dx.doi.org/10.1021/ic5004319 | Inorg. Chem. 2014, 53, 5229−5239

$ZnCl_2$ salts in Millipore water at 3 mM. Zinc concentrations were estimated by titrations using EDTA (5 mM) at pH 4.5 and xylenol as a colorimetric indicator. Extensive information is provided in the Supporting Information about the titrations and methods used to characterize the metal complexes.

RESULTS

Syntheses of the D-Pen-Based Tripodal Scaffolds L^4 and L^5. The tripodal scaffolds L^4 and L^5 were obtained by coupling 3 equiv of D-Pen ester or amide units on the trivalent NTA template, as previously described for L^1 and L^2 (Figure 2). The procedures used for the syntheses of L^4 and L^5 and the corresponding characterizations are reported in the Supporting Information.

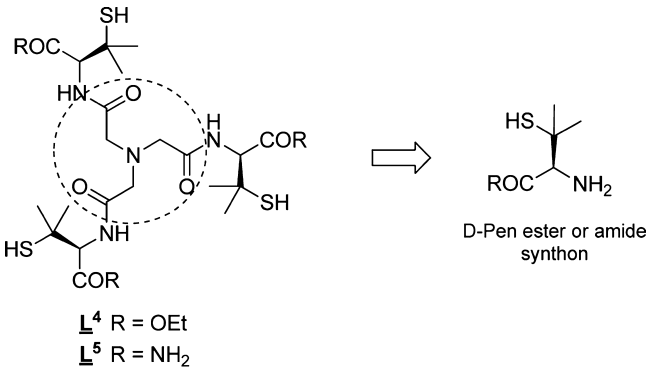

Figure 2. Synthetic strategy.

L^4 (Ester). The strategy previously used[27,28] to synthesize the ester derivative of cysteine with *p*-toluenesulfonate in ethanol was first attempted to obtain the D-Pen ester synthon.[45] This esterification reaction does not occur with the substrate H-D-Pen(Trt)-OH, whatever the temperature and the reaction time. Trityl cleavage is systematically observed. The steric hindrance due to the *gem*-dimethyl group is probably responsible for the enhanced lability of the trityl groups and the lack of reactivity of the carboxylic acid function. Therefore, another esterification method was selected. The esterification reaction was performed under basic conditions to avoid trityl deprotection, using cesium carbonate as a base and ethyl bromide as an electrophilic agent.[46] To prevent side reactions on the free amine, the protected Fmoc-D-Pen(Trt)-OH derivative was used as a starting material. Thus, the ester derivative Fmoc-D-Pen(Trt)-OEt (**1**) was obtained with 92% yield (step a, Scheme 1). Then, the Fmoc group was cleaved using triethylamine (step b, Scheme 1) to give the compound D-Pen(Trt)-OEt (**2**) with 60% yield.[47] The synthon D-Pen(Trt)-OEt (**2**) was then coupled to the NTA template (step c, Scheme 1), as previously described for the cysteine-based tripodal scaffolds.[27,28] This reaction leads to the trityl-protected tripod NTA[D-Pen(Trt)-OEt]$_3$ (**3**) in 72% yield. Eventually, the trityl groups are cleaved in acidic medium (step d, Scheme 1) to provide L^4 (36% yield, four steps, 14% global yield).

L^5 (Amide). The strategy used to synthesize L^4 was applied to the amide-functionalized D-Pen-based scaffold L^5 as depicted in Scheme 2. The D-Pen amide synthon was obtained by a two-step aminoacylation sequence. The first step (step a, Scheme 2) consisted of an NHS activation[48,49] of Fmoc-D-Pen(Trt)-OH to afford the compound Fmoc-D-Pen(Trt)-ONHS (**4a**) in 92% yield. The activated acid (**4a**) was then involved in an aminoacylation reaction with ammonium hydroxide[50] (step b, Scheme 2) to provide the compound Fmoc-D-Pen(Trt)-NH_2 (**4b**; 98%), which was Fmoc-deprotected to afford the compound D-Pen(Trt)-NH_2 (**5**; step c, Scheme 2, 78%). The compound **5** was then involved in a coupling reaction with the NTA template to provide the trityl-protected tripodal NTA[D-Pen(Trt)-OEt]$_3$ **6** (step d, Scheme 2, 98%). Eventually, the trityl groups were cleaved under acidic conditions to provide L^5 (step e, Scheme 2, 35%, five steps, 24% global yield).

As expected, these two novel ligands derived from D-Pen are more lipophilic than their cysteine analogues L^1 and L^2. In particular, the ester compound L^4 is not soluble in water at physiological pH and addition of acetonitrile was revealed to be necessary for all the studies. On the other hand, compound L^5, which is the relevant chelator for in vivo studies, since the ester function of L^4 may hydrolyze in the intracellular medium, is

Scheme 1. Synthesis of the Tripodal D-Penicillamine-Based Ligand L^4 (Ester)[a]

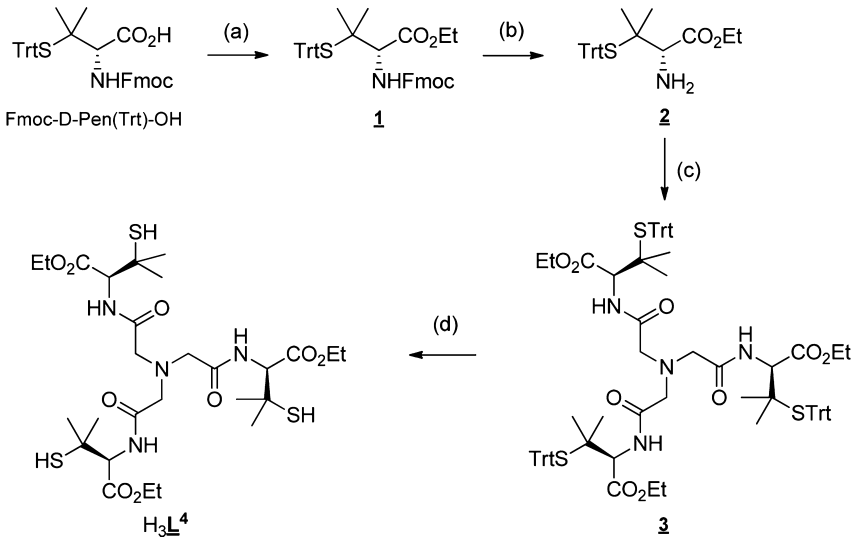

[a]Experimental conditions: (a) Cs_2CO_3, EtBr, DMF, room temperature, 3 h, 92%; (b) NEt_3/DMF (5/5, v/v), room temperature, 4 h, 60%; (c) NTA, EDC, HOBt, room temperature, DMF, 4 h, 72%; (d) TFA/TES, DCM, room temperature, 2 h, 36% (four steps, 14% global yield).

dx.doi.org/10.1021/ic5004319 | Inorg. Chem. 2014, 53, 5229−5239

Scheme 2. Synthesis of the Tripodal D-Penicillamine-Based Ligand L^5 (Amide)[a]

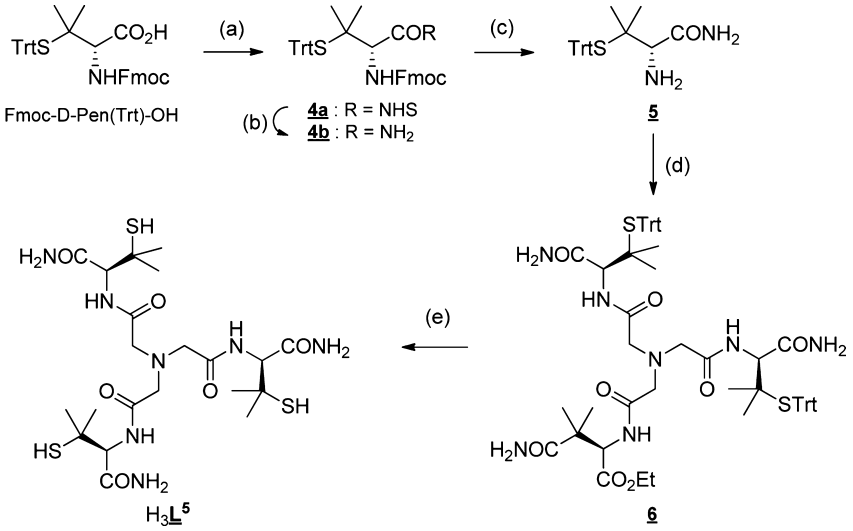

[a]Experimental conditions: (a) NHS, room temperature, then EDC, 0 °C, ACN, room temperature, 16 h, 92%; (b) NH_3 30%, ACN, room temperature, 1 h, 98%; (c) NEt_3, ACN, room temperature, 7.5 h, 78%; (d) NTA, EDC, HOBt, room temperature, ACN, 16 h, 98%; (e) TFA/TES, DCM, room temperature, 2 h, 35% (five steps, 24% global yield).

fully soluble in water at pH 7.4. In the following studies with L^5, acetonitrile was added only to preserve the oxidation state of Cu(I).

Cu(I) Complexes with the Ligand L^5. Physicochemical studies conducted on Cu(I) complexes with L^5 all point to the formation of two types of complexes: the first has a 1:1 stoichiometry and corresponds to the mononuclear species CuL^5, and the second displays an overall 2:1 stoichiometry $(Cu_2L^5)_z$.

These two complexes were first evidenced by mass spectrometry. Spectra acquired in the negative mode display two major ions: m/z 642 for $[L^5 + H + Cu]^-$, which is characteristic of a mononuclear Cu complex, and m/z 704 for $[L^5 + 2Cu]^-$, which most likely originates from a $(Cu_2L)_z$ type cluster. The corresponding spectra are reported in Figures S1 and S2 in the Supporting Information.

The binding of Cu(I) has also been investigated by UV spectroscopy. The spectra recorded for the titration of L^5 with $Cu(CH_3CN)_4PF_6$ are depicted in Figure 3. They display the appearance of a band centered at 262 nm, the intensity of which increases with the Cu(I) concentration. This band is characteristic of charge transfer transitions (LMCT) from thiolates to Cu(I).[51] An extra band appears at lower energy (315 nm) and accounts for formally spin forbidden 3d to 4s metal cluster centered transitions brought about by Cu- - -Cu interactions in clusters.[52] As shown in the inset of Figure 3, two changes of level appear on the curves at 262 and 315 nm for 1 and 2 equiv of Cu(I). From these data, it can be deduced that both the mononuclear complex CuL^5 and polymetallic $(Cu_2L^5)_z$ species form in solution, with the cluster molecularity z undetermined at this step of the study.

CD titrations, depicted in Figure 4, correlate the data obtained by UV spectroscopy: from 0 to 1 equiv of Cu(I) (blue curves in Figure 4), two positive bands (250 nm, 270 nm) and one negative band (225 nm) regularly increase with a well-defined isodichroic point at 240 nm. Above 1 equiv of Cu(I), the 250 nm centered band completely collapses, whereas the 270 nm centered band continues to increase until 2 equiv of Cu(I) was added. Above 2 equiv of Cu(I), all of the spectra

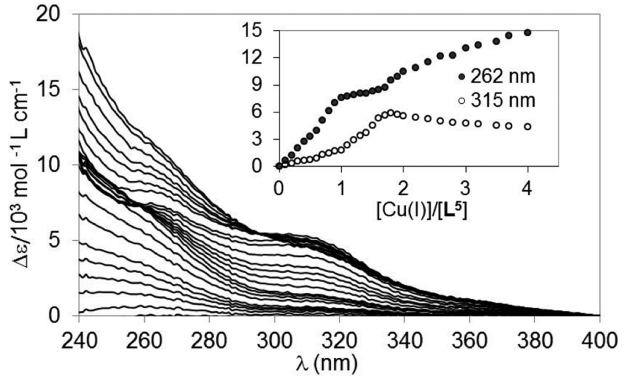

Figure 3. UV titration of L^5 (61 μM) at pH 7.4 (20 mM phosphate buffer/MeCN, 9/1 v/v) with Cu(I) (0–4 equiv). The inset gives the difference spectra $\Delta\varepsilon = \varepsilon(CuL^5) - \varepsilon(L^5)$ at 262 nm (LMCT) and at 315 nm (cluster transitions), respectively.

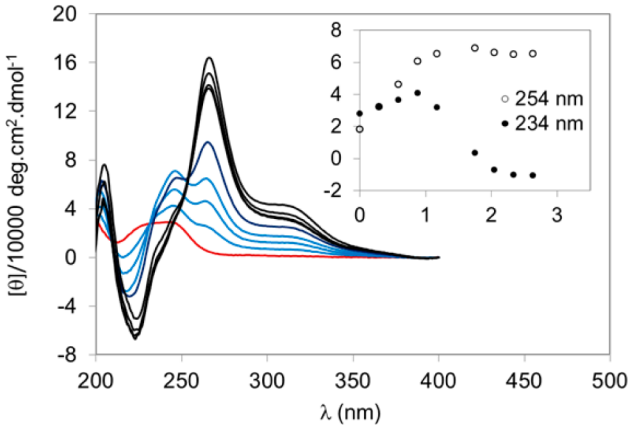

Figure 4. CD titration of L^5 (46 μM) at pH 7.4 (20 mM phosphate buffer/MeCN, 9/1 v/v) with Cu(I) (0–2.5 equiv): (red) free L^5; (blue) 0.25–1 equiv of Cu(I); (black) 1.5–2.5 equiv of Cu(I).

dx.doi.org/10.1021/ic5004319 | Inorg. Chem. 2014, 53, 5229–5239

recorded are superimposed. The first band centered at 250 nm indicates the formation of the mononuclear complex, whereas the second band centered at 270 nm prevails when the $(Cu_2L^5)_z$ cluster become the major species in solution.

NMR spectra are very informative about the two species formed. The titrations of L^5 with Cu(I) followed by NMR have been performed in a 20 mM phosphate buffer in D_2O/MeCN (9/1, v/v) mixture with 1 mM ligand concentration and are shown in Figure 5. The spectrum of the ligand indicates a C_3-

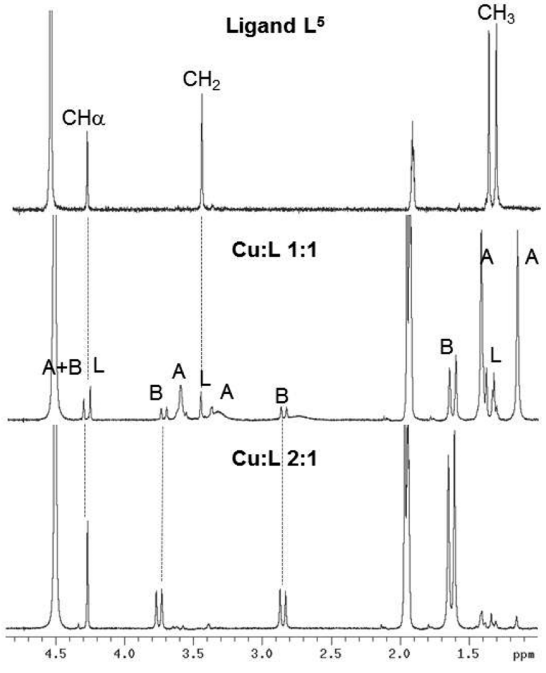

Figure 5. 400 MHz ^{1}H NMR at 298 K of L^5 (1 mM) at pD 7.4 (20 mM phosphate buffer in D_2O/CD_3CN, 9/1 v/v) with 1 equiv of Cu(I) (67% A, 22% B, 11% L) or 2 equiv of Cu(I) (100% B).

symmetric species with three distinct proton signals: the 18 protons of the two D-Pen methyl groups at 1.45 and 1.38 ppm, the 6 methylene protons of the NTA scaffold at 3.5 ppm, and the 3 α-CH protons of the D-Pen units at 4.4 ppm. When aliquots of Cu(I) in CD_3CN are added to the sample, the signals of three different C_3-symmetric species coexist and are in slow exchange on the NMR time scale. Those signals correspond to the free ligand (L), the mononuclear complex CuL^5 (A), and the polymetallic species $(Cu_2L^5)_z$ (B). The signals of A appear first, for 0.25 equiv of Cu(I) added. The signals of B are detected above 0.5 equiv of Cu(I) and regularly increase at the expense of signals L and A until 2 equiv of Cu(I) is added. As depicted in Figure 5, for 2 equiv of Cu(I) added, only the signals B are visible in the spectrum, evidencing the existence of the only remaining $(Cu_2L^5)_z$ species in solution. One noticeable feature is the splitting of the signal of the methylene protons of the NTA scaffold into an AB system which is very well-defined in $(Cu_2L^5)_z$, indicating the rigidity of the polymetallic Cu(I) complex.

All together UV, CD, and NMR spectroscopy and mass spectrometry evidence the formation of two Cu(I) complexes: CuL^5 and a $(Cu_2L^5)_z$ cluster.

Cu(I) Complexes with the Ligand L^4. In contrast, the same experiments run with the ester derivative L^4 point to the formation of only one complex, with an overall 2:1 stoichiometry. Indeed, the UV titration displays the two bands seen previously for L^5 but with only one change of level for 2 equiv of Cu(I) (Figure 6), indicating the formation of only one complex, namely $(Cu_2L^4)_z$.

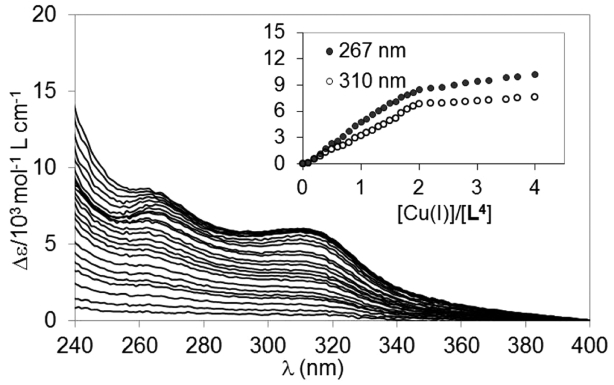

Figure 6. UV titration of L^4 (45 μM) at pH 7.4 (20 mM phosphate buffer/MeCN, 9/1, v/v) with Cu(I) (0–4 equiv). The inset gives the difference spectra $\Delta\varepsilon = \varepsilon(CuL^4) - \varepsilon(L^4)$ at 267 nm (LMCT) and at 310 nm (cluster transitions), respectively.

CD titrations, depicted in Figure S6 in the Supporting Information, also show the growth of only one positive band centered at 270 nm, which regularly increases during the titration until 2 equiv of Cu(I) is added. The mass spectra do not show the 1:1 species but a signal at m/z 791 for $[L^4 + 2Cu]^-$, which originates from a $(Cu_2L)_z$ cluster. The corresponding spectrum is reported in Figure S3 in the Supporting Information. The formation of only one copper complex is finally demonstrated by the NMR data shown in Figure S7 in the Supporting Information. A less polar solvent, phosphate buffer in D_2O/MeCN (5/5, v/v), has been used for L^4, not soluble at 1 mM in 20 mM phosphate buffer in a D_2O/MeCN (9/1, v/v) mixture. The spectrum of the free ligand is characteristic of a C_3-symmetric molecule with the 9 methyl protons of the ester group at 1.2 ppm, the 18 protons of the two D-Pen methyl groups at 1.4 and 1.5 ppm, the 6 methylene protons of the NTA scaffold at 3.4 ppm, the 6 methylene protons of the ester group partially hidden by the residual water solvent signal, and the 3 α-CH protons of the D-Pen units at 4.5 ppm. During the titration with Cu(I), only two sets of signals coexist in the spectra: the signals (L) for the free ligand protons and the signals (C) for the protons of the $(Cu_2L^4)_z$ cluster species (Figure S7, Supporting Information). The signals C increase with Cu(I) addition at the expense of signals L. At the end of the titration, for 2 equiv of Cu(I) added, only signals C can be seen in the spectrum. As for $(Cu_2L^5)_z$, a well-defined AB system accounts for the methylene protons of the NTA scaffold in a rigid complex.

These experiments demonstrate that the ester derivative L^4, which is bulkier than the corresponding amide ligand L^5, cannot accommodate the mononuclear complex in solution and thus forms exclusively a $(Cu_2L^4)_z$ species.

Molecularities of the Cu(I) Complexes. NMR is a powerful tool to infer the molecularities of species in solution. Indeed, diffusion coefficients measured by NMR spectroscopy using pulsed field-gradient spin echo (PFGSE) sequences are characteristic of the presence of unimolecular, bimolecular, or oligomeric species in solution.[53−55] The diffusion constant D can be related to the hydrodynamic radii of the molecules via the Stokes−Einstein equation (1), where k is the Boltzmann

dx.doi.org/10.1021/ic5004319 | Inorg. Chem. 2014, 53, 5229−5239

$$D = \frac{kT}{6\pi\eta r_H} \quad (1)$$

constant, T the absolute temperature, η the viscosity, and r_H the hydrodynamic radius of the diffusing species, considered as a hypothetical hard sphere that diffuses with the same speed as the particle under examination. Thus, the determination of D by diffusional NMR for shape-similar complexes and ligands is an efficient tool for deducing the molecular mass of an unknown species (i, molar mass M_i) in solution, when a reference compound (r, molar mass M_r) is measured under the same conditions. Indeed, eq 2 allows the determination of the unknown molar mass M_i of interest.

$$\frac{D_i}{D_r} = \sqrt[3]{\frac{M_r}{M_i}} \quad (2)$$

Experimental masses (M_{exptl}) derived from eq 2, taking the free ligand in the same solvent as a reference compound and theoretical masses calculated from the compound's formulas, are reported in Table 1. These data confirm that the signals of

Table 1. Diffusion Coefficients Measured by PFGSE ^{1}H NMR at 298 K for Metallic Species Formed with L^4 and L^5 at pD 7.4[a]

	D (10^{10} m^2 s^{-1} mol^{-1})	M_{exptl} (g/mol)[b]	M_{theor} (g/mol)[c]
L^4	3.90(9)		669
$(Cu_2L^4)_2$	2.95(7)	1550(200)	1586
ZnL^4	3.70(1)	780(60)	731
L^5	3.02(9)		582
CuL^5	2.86(6)	685(90)	642
$(Cu_2L^5)_2$	2.36(9)	1220(220)	1412

[a]Diffusion coefficient measured in 20 mM phosphate buffer in D_2O/CD_3CN (9/1 v/v for L^5 and 5/5 v/v for L^4). Experimental errors in the last digit are indicated in parentheses. [b]Molecular mass calculated with eq 2, the reference compound being the free ligand in the same solvent. [c]Molecular mass calculated with the chemical formula of the species.

A detected in the ^{1}H NMR spectra with the amide derivative L^5 correspond to the Cu(I) mononuclear complex CuL^5. In addition, this set of measurements allows the determination of the two cluster molecularities, detected in the ^{1}H NMR spectra as C for L^4 and B for L^5. Both clusters show diffusion coefficients characteristic of a molecularity $z = 2$ and are thus $(Cu_2L)_2$ species i.e., Cu_4S_6-type clusters. It is quite interesting to notice that the analogous cysteine-based scaffold L^1 forms a cluster with a higher nuclearity ($z = 3$) and a Cu_6S_9 core.[27,28] These data suggest that analogous ligands tend to form similar metallic species in solution with different molecularities depending on the steric hindrance of the pseudopeptide scaffolds.

Copper K-Edge X-ray Absorption Spectroscopy. Cu K-edge X-ray Absorption spectroscopy (XAS) spectra were collected at the BM30B FAME beamline at the European Synchrotron Radiation Facility (ESRF, Grenoble, France) at low temperature (10 K).[56,57] They confirmed the speciation deduced from other spectroscopic data and provided significant complementary information about the Cu(I) species formed in solution. The samples analyzed by XAS are given in Table 2. The L^5 concentration was around 3 mM, with Cu(I) varying

Table 2. Samples Analyzed by XAS in a Phosphate Buffer (100 mM, pH 7.4)/Glycerol/Acetonitrile (7/2/1, v/v/v) Mixture[a]

L	sample	[Cu]/[L]	[Cu] (mM)	[L] (mM)
L^4	4A	1	0.566	0.569
	4B	1.5	0.838	0.562
	4C	2	1.104	0.554
L^5	5A	0.17	0.5	2.91
	5B	0.92	2.5	2.71
	5C	1.64	3.5	2.6
	5D	1.8	4.5	2.5
	5E	1.99	4.83	2.42

[a]Note that lower [L^4] (mM) concentrations were used due to the lack of solubility of L^4 in the solvent because of its relatively apolar character in comparison to L^5.

from 0.17 to 2 equiv. The lower solubility of L^4 prevented the preparation of samples more concentrated than 0.56 mM. Furthermore, the Cu(I) content could not be decreased below 1 equiv for XAS sensitivity reasons.

The spectra of the Cu(I) complexes with L^4 and L^5 are compared in Figure 7. The peaks are centered at 8982 eV,

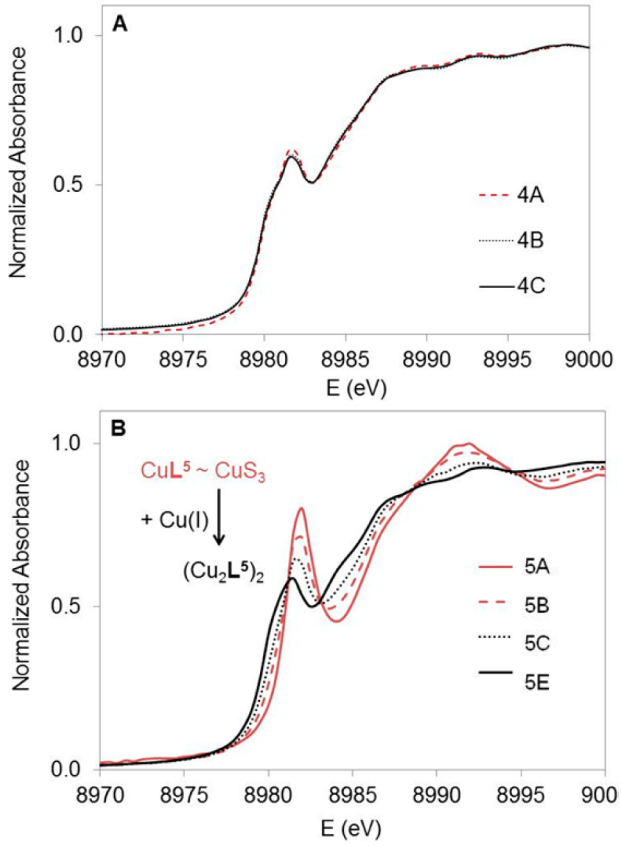

Figure 7. Normalized Cu edge spectra of Cu(I) complexes with (A) L^4 and (B) L^5.

which accounts for the existence of Cu(I) species. In Figure 7B, it clearly appears that two species are coexisting during the titration of L^5 with Cu(I), as evidenced by the existence of several isosbestic points (8981, 8984, 8988, and 8994 eV).

In addition, the peak centered at 8982 eV linearly decreases with Cu(I) addition, accounting for the formation of the polymetallic species at the expense of the mononuclear

dx.doi.org/10.1021/ic5004319 | Inorg. Chem. 2014, 53, 5229−5239

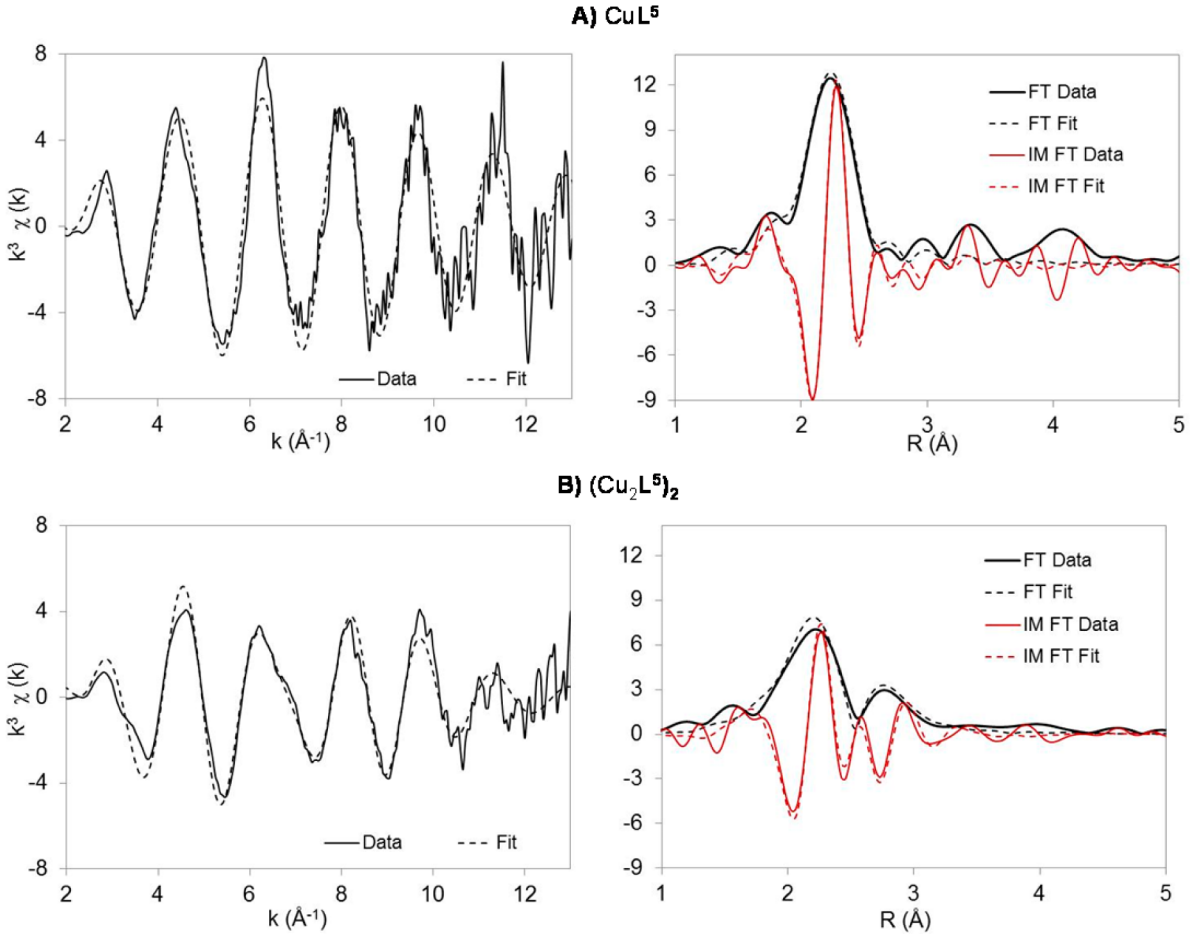

Figure 8. XAS data for (A) the mononuclear complex Cu$\mathbf{L}^5$ (sample 5A) and (B) the cluster $(Cu_2\mathbf{L}^5)_2$(sample 5F): (left) spectra of the k^3-weighted EXAFS experimental data and corresponding fit; (right) Fourier transforms of the k^3-weighted EXAFS experimental data and corresponding fit. FT and IM FT are the magnitude and imaginary part of Fourier transforms, respectively. Solid lines indicate experimental data, and dotted lines indicate fits.

complex Cu$\mathbf{L}^5$. This peak corresponds to 1s−4p Cu(I)-centered transitions, the intensity of which evidence the coordination geometry adopted around the central Cu(I) ions.[58] On the other hand, the three spectra recorded for $\mathbf{L}^4$ complexes (Figure 7A) are superimposable, whatever the Cu to $\mathbf{L}^4$ ratio. Moreover, they are very similar to the spectrum of $(Cu_2\mathbf{L}^5)_2$, which is consistent with the exclusive formation of the polymetallic complex $(Cu_2\mathbf{L}^4)_2$.

Comparisons with previous XAS data acquired with cysteine derivatives are consistent with tris(thiolato) environments in either mononuclear species or cluster complexes.[42,59] This was confirmed by the extended X-ray absorption fine structure (EXAFS) analysis.

EXAFS Analyses. To characterize the Cu(I) species formed in solution and refine the structure of the coordination spheres around the Cu(I) ion in each case, the EXAFS domains of the XAS spectra were then looked into. The EXAFS data of the mononuclear complex Cu$\mathbf{L}^5$ were analyzed in sample 5A with low Cu(I) concentration. The cluster $(Cu_2\mathbf{L}^5)_2$ was investigated in sample 5F, which contains 2 equiv of Cu(I). Samples 5A and 5F were shown by ^{1}H NMR to contain only the mononuclear adduct and polymetallic adducts, respectively. The cluster $(Cu_2\mathbf{L}^4)_2$ could be analyzed in each of the three samples (4A−C), which show identical XAS and EXAFS spectra, since this is the only species formed with $\mathbf{L}^4$ under our conditions. The results are presented here with sample 4A.

Two structural models were applied to fit the EXAFS data using the Horae package,[60] including ATHENA for the data extraction and ARTEMIS for the shell fitting. The first model (coordinate-based model) was derived from the atomic coordinates of sulfur and copper atoms in the $[Cu_4(CH_3S^-)_6]^{2-}[(C_3H_7)_4N^+]_2$ cluster described by Baumgartner et al.[61] On the basis of this structure, the atomic coordinates of Cu(1), S(1), S(2), and S(3) were used in Atoms (Artemis module) for the mononuclear complex, as a starting point for the structural fitting. For the clusters, data were fitted using a model based on the whole set of Cu and S coordinates from the same Baumgartner et al. structure, since in this case one copper atom is surrounded by three S and three Cu atoms, as expected for the L-based Cu(I) clusters. The second structural model (tetrahedral-based model) simply uses Cu surrounded by atom shells in a tetrahedral geometry (see the Supporting Information for further information). In the fits presented in the following the coordination number was set to three sulfurs since using either two sulfur atoms or three nonequivalent sulfur atoms in the first theoretical shell returns bad results and nonphysical parameter values.

Mononuclear Complex Cu$\mathbf{L}^5$. The EXAFS fitting results obtained for the mononuclear complex Cu$\mathbf{L}^5$ are depicted in Figure 8A. Both the coordinate-based and the tetrahedral-based models return good fits of the data collected. The quantitative results are reported in Table 3. The three sulfur−copper

dx.doi.org/10.1021/ic5004319 | Inorg. Chem. 2014, 53, 5229−5239

Table 3. EXAFS Fitting Results[a]

complex	sample	model	3 × Cu−S	$\sigma(S)^2$	3 × Cu−Cu	$\sigma(Cu)^2$	ΔE	χ_n^2	R
CuL^5	5A	coordinates	2.23	5(1)			3(2)	24	3.0
CuL^5	5A	tetrahedral	2.23	4(1)			4(2)	24	3.0
$(Cu_2L^5)_2$	5F	coordinates	2.22	8(1)	2.66, 2.74, 2.83	10(3)	4(2)	91	6.0
$(Cu_2L^5)_2$	5F	tetrahedral	2.22	8(1)	2.75	15(4)	4(2)	111	6.7
$(Cu_2L^4)_2$	4A	coordinates	2.22	7(1)	2.62, 2.68, 2.77	8(2)	4(3)	31	6.7
$(Cu_2L^4)_2$	4A	tetrahedral	2.22	7(1)	2.69	13(2)	4(2)	26	6.1

[a]Distances are given in Å with errors of 0.01 and 0.02 for Cu−S and Cu−Cu distances, respectively. Other experimental errors in the last digit are indicated in parentheses. Debye−Waller factors (σ^2) are given in $Å^2 \times 10^3$. The threshold energy shift ΔE is given in eV. χ_n^2 and R (%) are the reduced χ^2 value and the R factor of the fit, respectively. The "coordinates" model uses the atomic coordinates of the cluster $[Cu_4(CH_3S^-)_6]^{2-}[(C_3H_7)_4N^+]_2$ described by Baumgartner et al.[61] Only the atomic coordinates of Cu(1), S(1), S(2), and S(3) were used to fit the mononuclear complex, whereas the whole set of Cu and S atomic coordinates was used to fit the clusters. The "tetrahedral" model simply uses Cu surrounded by atoms in a tetrahedral geometry.

distances were found to be almost equal: Cu−S ≈ 2.23 Å. This distance belongs to the characteristic distance range reported for symmetric CuS_3 compounds (~2.22−2.26 Å) studied by either XAS or crystallography.[30−35,42,62] Consequently, these data confirm that $\mathbf{L^5}$ forms a mononuclear complex with C_3-symmetric CuS_3 coordination. Moreover, the C_3-symmetric species detected in the NMR spectra recorded at 298 K are not average signals of dissymmetric species, as observed previously for mercury complexes of $\mathbf{L^1}$ and $\mathbf{L^2}$.[41] It is quite interesting to notice that the cysteine-based ligands $\mathbf{L^1}$ and $\mathbf{L^2}$ and the D-Pen-based ligand $\mathbf{L^5}$, all derived from the same NTA template, form trigonal-planar mononuclear complexes with identical Cu−S distances (Cu−S ≈ 2.23 Å),[42] despite the steric hindrance of the *gem*-dimethyl groups of the three D-Pen units in $\mathbf{L^5}$.

Clusters. The EXAFS fitting results obtained for the clusters $(Cu_2\mathbf{L^5})_2$ are depicted in Figure 8B. A beat between 6 and 8 $Å^{-1}$ on the wave vector *k*-space curve effectively accounts for the presence of Cu- - -Cu interactions in the $(Cu_2\mathbf{L^5})_2$ species formed in solution. Such a beat originates from waves out of phase from different shells of atoms.[61] The corresponding Cu- - -Cu peak at ≈2.7 Å can be observed in the distance R-space in Figure 8B. Analogous graphs were obtained for the cluster $(Cu_2\mathbf{L^4})_2$ (Figure S8 in the Supporting Information). Again both the coordinate-based model and the tetrahedral-based model return good fits of the data collected. The quantitative results are reported in Table 3. The distances Cu−S ≈ 2.22 Å and Cu- - -Cu ≈ 2.7 Å were found to be in accordance with the values given in the literature for several Cu(I) proteins,[30−33] in particular metallothioneins (MTs),[34,35,62] and some inorganic model clusters[61] organized on CuS_3 cores which interact with one to three nearby copper atoms in either Cu_4S_6 or Cu_6S_9 clusters. The Cu- - -Cu distances obtained with the coordinate-based model are not equal (~2.66−2.83 Å; see Table 3), but the resolution expected for these second-shell atoms is too low (~0.1 Å)[63] to allow a discrimination between such close distances. Therefore, the tetrahedral-based model, which sets the three Cu atoms at the same distance (2.7 Å) from the central Cu is preferred. The most striking features are probably the short Cu−S distances measured in the two clusters (Cu−S ≈ 2.22 Å). Indeed, these latter distances are significantly shorter than that previously measured in the $(Cu_2\mathbf{L^1}/\mathbf{L^2})_3$ polymetallic species formed with the cysteine derivatives, with Cu−S distances of 2.26 Å.

Affinity for Cu(I). Considering the species identified in the previous sections, the thermodynamic equilibria for the formation of Cu(I) complexes with $\mathbf{L^5}$ are described by eqs 3 and 4, whereas only eq 4 is necessary for $\mathbf{L^4}$.

$$Cu(I) + L = CuL \quad \beta_{11} \tag{3}$$

$$4Cu(I) + 2L = (Cu_2L)_2 \quad \beta_{42} \tag{4}$$

The conditional stability constants at pH 7.4 were determined by UV spectroscopy in the presence of bathocuproine disulfonate (BCS), which forms the orange complex $Cu(BCS)_2^{3-}$ of known stability.[33] The values are reported in Table 4. It appears that the formation constant value for CuL^5

Table 4. Conditional Stability Constants of Cu(I) and Zn(II) Complexes Formed with L^4 and L^5 at pH 7.4[a]

complex	$\log \beta_{11}^{pH\ 7.4}$	$\log \beta_{42}^{pH\ 7.4}$	$\log(\beta_{11}^{Cu}/\beta_{11}^{Zn})$
$(Cu_2L^4)_2$	17.3[b]	71.5(1)	
CuL^5	16.2(1)		
$(Cu_2L^5)_2$		68(1)	
ZnL^4	6.5(1)		10.8
ZnL^5	6.3(1)		9.9

[a]Conditional stability constants with Cu(I) were measured in 20 mM phosphate buffer pH 7.4/MeCN (9/1 v/v) and conditional stability constants with Zn(II) in 20 mM Hepes buffer pH 7.4/MeCN (9/1, v/v). Experimental errors in the last digit are indicated in parentheses. [b]Constant calculated for the formation of an assumed CuL^4 complex.

($\log \beta_{11}^{pH\ 7.4} = 16.2$) is significantly lower than those found for the cysteine derivatives $\mathbf{L^1}$ and $\mathbf{L^2}$ (19.2 and 18.8, respectively).[27,28,42] This difference can be assigned to the steric hindrance due to the *gem*-dimethyl groups near the coordinating thiolates in the D-Pen derivative. However, $\mathbf{L^5}$ can compete with several Cu(I) proteins in cells, since the affinities reported for Cu(I) proteins are in the range $\log \beta_{11}^{pH\ 7.4} = 15-20$.[25,64,65] The two clusters $(Cu_2\mathbf{L^4})_2$ and $(Cu_2\mathbf{L^5})_2$ display large stabilities of the same order of magnitude. Therefore, these measurements demonstrate that both $\mathbf{L^4}$ and $\mathbf{L^5}$ bind Cu(I) with affinities which make them potential intracellular Cu(I) chelators for detoxification. However, for the applications in vivo, information about the selectivities is required to ensure that Cu can be bound in vivo without altering the homeostasis of the essential metal ion Zn(II). This is why the complexation properties with Zn(II) have been investigated.

Zn(II) Complexation and Selectivity. The titrations of $\mathbf{L^4}$ and $\mathbf{L^5}$ with Zn(II) followed by UV and CD spectroscopy are reported in Figure 9 and Figure S9 (Supporting Information) for $\mathbf{L^4}$ and $\mathbf{L^5}$, respectively. These data show the exclusive formation of the mononuclear species ZnL, which is also

dx.doi.org/10.1021/ic5004319 | Inorg. Chem. 2014, 53, 5229−5239

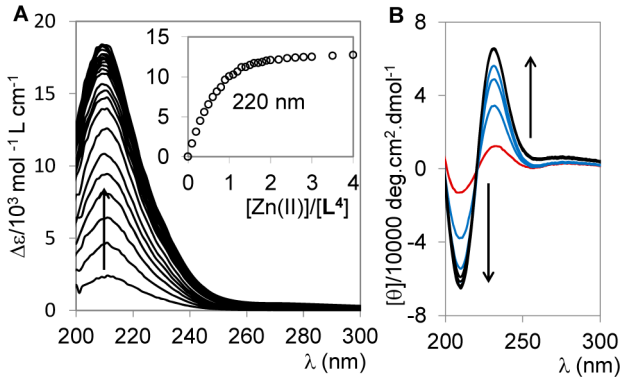

Figure 9. Titrations of $\mathbf{L}^4$ (ca. 45 μM) at pH 7.4 (20 mM phosphate buffer/MeCN, 9/1 v/v) with Zn(II): (A) UV titration with 0−4 equiv of Zn(II); (B) CD titration with 0−2 equiv of Zn(II) (color scheme: red, free ligand; blue, 0.25−0.75 equiv of Zn; black, 1−2 equiv of Zn).

evidenced in the ES-MS spectra (see Figures S4 and S5 in the Supporting Information). For instance, the CD titration of $\mathbf{L}^4$ with Zn(II) presented in Figure 9B shows a saturation at 1 equiv of Zn(II) with the presence of an isodichroic point. The molecularity of these complexes was confirmed by the diffusion coefficients measured by ^{1}H NMR spectroscopy, as seen in Table 1. In contrast, the cysteine derivatives $\mathbf{L}^1$ and $\mathbf{L}^2$ have been found to form mixtures of monomolecular Zn**L** and bimolecular $(\mathrm{Zn}\mathbf{L})_2$ complexes to satisfy the preferred tetrahedral coordination of Zn in ZnS_4 binding sites.[28] This difference can be reasonably attributed to the steric hindrance of the two D-Pen derivatives, which cannot accommodate the tetrahedral environment around the Zn(II) ion. It is also highly probable that water or acetonitrile completes the coordination spheres of the Zn**L** species formed with $\mathbf{L}^4$ and $\mathbf{L}^5$. A similar effect was previously observed on comparing cysteine and penicillamine ligands in Co(II) maquettes.[40]

The stability of the Zn(II) complexes was measured using zincon (ZI) as a competitor.[66] As seen in Table 4, low affinities for Zn(II) are found for the two ligands, which are reasonably related to their inability to provide tetrahedral Zn(II) environments.

Consequently, it can now be confirmed that the new tripodal ligands $\mathbf{L}^4$ and $\mathbf{L}^5$ selectively bind the Cu(I) ion, which is of great importance for applications in vivo.

DISCUSSION

This work was aimed at developing novel Cu(I) chelating agents derived from D-Pen, which is the drug mostly used currently to treat Wilson's disease. Although the mechanism of action of D-Pen in vivo has not been fully demonstrated, it is expected to act as a reductive chelator that reduces Cu(II) to Cu(I) and binds Cu(I) either in a five-membered chelate ring involving the nitrogen and sulfur donors of the ligand or in a Cu(I)−thiolate polymer.[67] The stability constant of the Cu(I) complex with D-Pen was estimated in a chloride-rich medium: $\log \beta_{10} \approx 12$.[68] Considering the promising chelating properties of tripodal pseudopeptides based on three converging cysteine moieties,[27,28] three D-Pen units were coupled to nitrilotriacetic acid to obtain the two D-Pen derivatives $\mathbf{L}^4$ and $\mathbf{L}^5$. In contrast to D-Pen, these two compounds are sulfur donors only, since the amines of the three D-Pen building blocks are involved in peptide bonds.

Investigation of their Cu(I) chelating properties evidenced a significant effect of the neighboring group carried by the D-Pen carbonyl functions. A subtle modification at the periphery of the pseudopeptides such as replacement of ethyl esters in $\mathbf{L}^4$ by amide in $\mathbf{L}^5$ significantly affects the Cu(I) complex speciation. Indeed, all spectroscopic and analytical tools point to the formation of a unique and well-defined cluster with $\mathbf{L}^4$, namely $(\mathrm{Cu}_2\mathbf{L}^4)_2$, whereas $\mathbf{L}^5$ gives two types of Cu(I) complexes. The mononuclear complex $\mathrm{Cu}\mathbf{L}^5$ is formed with an excess of the ligand and the cluster $(\mathrm{Cu}_2\mathbf{L}^5)_2$ with an excess of the metal. The two clusters show the same features with a molecularity $z = 2$ corresponding to a Cu_4S_6 core, which is found in many inorganic copper complexes with proteins[69] including MTs,[34,35,62] copper chaperones,[31,32] transcription factors,[30] and the intracellular domain of copper transporters.[33] Interestingly, EXAFS data prove systematically a trigonal-planar coordination around Cu(I) with sulfurs only and Cu−S distances (2.22−2.23 Å) characteristic of a CuS_3 geometry. Finally, these two novel ligands were demonstrated to bind Cu(I) tightly with affinities similar to those found in proteins and selectively with respect to Zn(II). The selectivity for Cu(I) with respect to Zn(II) is assigned to the inability of these bulky tripods to accommodate the preferred tetrahedral geometry of Zn(II).[70]

A comparison with the cysteine homologues $\mathbf{L}^1$ and $\mathbf{L}^2$ evidences a significant effect of the *gem*-dimethyl groups in $\mathbf{L}^4$ and $\mathbf{L}^5$. Since cysteine and penicillamine show similar basicities—pK_a =7.9 (Pen) and 8.3 (Cys)—this effect can be mainly attributed to the greater steric bulk at the C_β of D-Pen in comparison to cysteine. First, the influence of the neighboring ester or amide groups is a great deal more pronounced with the D-Pen derivatives than with the cysteine ones. Whereas $\mathbf{L}^1$ and $\mathbf{L}^2$ showed very similar speciation of their Cu(I) complexes, $\mathbf{L}^4$ and $\mathbf{L}^5$ exhibit different Cu(I) species formation with the exclusive presence of the cluster for the bulkier derivative $\mathbf{L}^4$. The most striking effect is probably the different molecularities of the clusters formed with the two series of ligands. The cysteine tripods form large clusters with a molecularity of 3 ($(\mathrm{Cu}_2\mathbf{L}^{1,2})_3$), which show very large signals on their ^{1}H NMR spectra indicative of their rapid interconversion on the NMR time scale. In contrast, the clusters formed with the more hindered D-Pen tripods are more compact with a molecularity of 2 ($(\mathrm{Cu}_2\mathbf{L}^{4,5})_2$). Moreover, the well-defined signals on the ^{1}H NMR spectra are consistent with rigid and well-defined complex structures. Finally, the steric hindrance due to the *gem*-dimethyl groups of the D-Pen derivatives is probably responsible for the slightly lower stability of their Cu(I) complexes in comparison to their cysteine homologues. In any event, they bind Cu(I) with affinities allowing competitions with many Cu binding sites in proteins, significantly higher than the affinity reported for D-Pen alone.[68]

It is likely that the D-penicillamine-based scaffolds could also provide efficient Cu(I) chelators in vivo. In order to validate the efficiency to chelate intracellular copper, the amide compound $\mathbf{L}^5$ is currently being functionalized to target the asialoglycoprotein receptors and to promote its internalization in hepatic cells. Since the D-Pen tripods are derived from non-natural amino acids, with a D absolute configuration, they are expected to be more stable and to display very interesting copper-chelating properties in vivo.

dx.doi.org/10.1021/ic5004319 | *Inorg. Chem.* 2014, 53, 5229−5239

■ ASSOCIATED CONTENT

Supporting Information

Full experimental section, details of the syntheses of ligands L^4 and L^5, physicochemical protocols, and data for the physicochemical studies. This material is available free of charge via the Internet at http://pubs.acs.org.

■ AUTHOR INFORMATION

Corresponding Author

*E-mail for P.D.: pascale.delangle@cea.fr.

Notes

The authors declare no competing financial interest.

■ ACKNOWLEDGMENTS

This research was supported by the "Agence Nationale pour la Recherche" (COPDETOX, ANR-11-EMMA-025), the "Fondation pour la Recherche Médicale" (grant DCM20111223043), and the Labex ARCANE (Grant ANR-11-LABX-0003-01). The authors acknowledge the European Synchotron Radiation Facility and FAME CRG beamline for provision of synchrotron radiation beamline and facilities. We thank Céline Rivaux for her technical help in the synthesis laboratory.

■ REFERENCES

(1) Holm, R. H.; Kennepohl, P.; Solomon, E. I. *Chem. Rev.* **1996**, *96*, 2239.
(2) Robinson, N. J.; Winge, D. R. *Annu. Rev. Biochem.* **2010**, *79*, 537.
(3) Kim, B. E.; Nevitt, T.; Thiele, D. J. *Nat. Chem. Biol.* **2008**, *4*, 176.
(4) Arnesano, F.; Banci, L.; Bertini, I.; Ciofi-Baffoni, S. *Eur. J. Inorg. Chem.* **2004**, 1583.
(5) Rosenzweig, A. C. *Acc. Chem. Res.* **2001**, *34*, 119.
(6) Tao, T. Y.; Gitlin, J. A. *Hepatology* **2003**, *37*, 1241.
(7) Guo, Y.; Nyasae, L.; Braiterman, L. T.; Hubbard, A. L. *Am. J. Physiol. Gastrointest. Liver Physiol.* **2005**, *289*, G904.
(8) Lutsenko, S.; Barnes, N. L.; Bartee, M. Y.; Dmitriev, O. Y. *Physiol. Rev.* **2007**, *87*, 1011.
(9) http://www.orpha.net.
(10) Brewer, G. J.; Askari, F. K. *J. Hepatol.* **2005**, *42*, S13.
(11) Sarkar, B. *Chem. Rev.* **1999**, *99*, 2535.
(12) Vilensky, J. A.; Redman, K. *Ann. Emerg. Med.* **2003**, *41*, 378.
(13) Walshe, J. M. *Mov. Disord.* **2006**, *21*, 142.
(14) Brewer, G. J.; Terry, C. A.; Aisen, A. M.; Hill, G. M. *Arch. Neurol.* **1987**, *44*, 490.
(15) Delangle, P.; Mintz, E. *Dalton Trans.* **2012**, *41*, 6359.
(16) Gateau, C.; Delangle, P. *Ann. N.Y. Acad. Sci.* **2014**, DOI: 10.1111/nyas.12379.
(17) Pujol, A. M.; Cuillel, M.; Renaudet, O.; Lebrun, C.; Charbonnier, P.; Cassio, D.; Gateau, C.; Dumy, P.; Mintz, E.; Delangle, P. *J. Am. Chem. Soc.* **2011**, *133*, 286.
(18) Rousselot-Pailley, P.; Seneque, O.; Lebrun, C.; Crouzy, S.; Boturyn, D.; Dumy, P.; Ferrand, M.; Delangle, P. *Inorg. Chem.* **2006**, *45*, 5510.
(19) Seneque, O.; Crouzy, S.; Boturyn, D.; Dumy, P.; Ferrand, M.; Delangle, P. *Chem. Commun.* **2004**, 770.
(20) Hamer, D. H. *Annu. Rev. Biochem.* **1986**, *55*, 913.
(21) Palacios, O.; Atrian, S.; Capdevila, M. *J. Biol. Inorg. Chem.* **2011**, *16*, 991.
(22) Stillman, M. J. *Coord. Chem. Rev.* **1995**, *144*, 461.
(23) Vasak, M.; Meloni, G. *J. Biol. Inorg. Chem.* **2011**, *16*, 1067.
(24) Calderone, V.; Dolderer, B.; Hartmann, H. J.; Echner, H.; Luchinat, C.; Del Bianco, C.; Mangani, S.; Weser, U. *Proc. Natl. Acad. Sci. U.S.A.* **2005**, *102*, 51.
(25) Faller, P. *Febs J.* **2010**, *277*, 2921.
(26) Gelinsky, M.; Vogler, R.; Vahrenkamp, H. *Inorg. Chem.* **2002**, *41*, 2560.
(27) Pujol, A. M.; Gateau, C.; Lebrun, C.; Delangle, P. *J. Am. Chem. Soc.* **2009**, *131*, 6928.
(28) Pujol, A. M.; Gateau, C.; Lebrun, C.; Delangle, P. *Chem. Eur. J.* **2011**, *17*, 4418.
(29) Jullien, A.-S. Thesis, Université Grenoble Alpes, Grenoble, France, 2013.
(30) Brown, K. R.; Keller, G. L.; Pickering, I. J.; Harris, H. H.; George, G. N.; Winge, D. R. *Biochemistry* **2002**, *41*, 6469.
(31) Pushie, M. J.; Zhang, L. M.; Pickering, I. J.; George, G. N. *Biochim. Biophys. Acta, Bioenerg.* **2012**, *1817*, 938.
(32) Voronova, A.; Meyer-Klaucke, W.; Meyer, T.; Rompel, A.; Krebs, B.; Kazantseva, J.; Sillard, R.; Palumaa, P. *Biochem. J.* **2007**, *408*, 139.
(33) Xiao, Z.; Loughlin, F.; George, G. N.; Howlett, G. J.; Wedd, A. G. *J. Am. Chem. Soc.* **2004**, *126*, 3081.
(34) George, G. N.; Byrd, J.; Winge, D. R. *J. Biol. Chem.* **1988**, *263*, 8199.
(35) George, G. N.; Winge, D.; Stout, C. D.; Cramer, S. P. *J. Inorg. Biochem.* **1986**, *27*, 213.
(36) Pujol, A. M.; Cuillel, M.; Jullien, A.-S.; Lebrun, C.; Cassio, D.; Mintz, E.; Gateau, C.; Delangle, P. *Angew. Chem., Int. Ed.* **2012**, *51*, 7445.
(37) Lee, K. H.; Cabello, C.; Hemmingsen, L.; Marsh, E. N.; Pecoraro, V. L. *Angew. Chem., Int. Ed.* **2006**, *45*, 2864.
(38) Peacock, A. F.; Stuckey, J. A.; Pecoraro, V. L. *Angew. Chem., Int. Ed.* **2009**, *48*, 7371.
(39) Chakraborty, S.; Touw, D. S.; Peacock, A. F.; Stuckey, J.; Pecoraro, V. L. *J. Am. Chem. Soc.* **2010**, *132*, 13240.
(40) Petros, A. K.; Shaner, S. E.; Costello, A. L.; Tierney, D. L.; Gibney, B. R. *Inorg. Chem.* **2004**, *43*, 4793.
(41) Pujol, A. M.; Lebrun, C.; Gateau, C.; Manceau, A.; Delangle, P. *Eur. J. Inorg. Chem.* **2012**, 3835.
(42) Jullien, A.-S.; Gateau, C.; Kieffer, I.; Testemale, D.; Delangle, P. *Inorg. Chem.* **2013**, *52*, 9954.
(43) Kamau, P.; Jordan, R. B. *Inorg. Chem.* **2001**, *40*, 3879.
(44) Riddles, P. W.; Blakeley, R. L.; Zerner, B. *Methods Enzymol.* **1983**, *91*, 49.
(45) Bolzati, C.; Mahmood, A.; Malago, E.; Uccelli, L.; Boschi, A.; Jones, A. G.; Refosco, F.; Duatti, A.; Tisato, F. *Bioconjugate Chem.* **2003**, *14*, 1231.
(46) Smith, N. D.; Goodman, M. *Org. Lett.* **2003**, *5*, 1035.
(47) Carpino, L. A.; Han, G. Y. *J. Org. Chem.* **1972**, *37*, 3404.
(48) Stasko, N. A.; Fischer, T. H.; Schoenfisch, M. H. *Biomacromolecules* **2008**, *9*, 834.
(49) Kim, J. E.; Cha, E. J.; Ahn, C. H. *Macromol. Chem. Phys.* **2010**, *211*, 956.
(50) Frey, B. L.; Corn, R. M. *Anal. Chem.* **1996**, *68*, 3187.
(51) Vasak, M.; Kagi, J. H. R.; Hill, H. A. O. *Biochemistry* **1981**, *20*, 2852.
(52) Pountney, D. L.; Schauwecker, I.; Zarn, J.; Vasak, M. *Biochemistry* **1994**, *33*, 9699.
(53) Waldeck, A. R.; Kuchel, P. W.; Lennon, A. J.; Chapman, B. E. *Prog. Nucl. Magn. Reson. Spectrosc.* **1997**, *30*, 39.
(54) Jershow, A.; Müller, N. *J. Magn. Reson.* **1997**, *125*, 372.
(55) Sinnaeve, D. *Concepts Magn. Reson. A* **2012**, *40A*, 39.
(56) Proux, O.; Biquard, X.; Lahera, E.; Menthonnex, J. J.; Prat, A.; Ulrich, O.; Soldo, Y.; Trevisson, P.; Kapoujyan, G.; Perroux, G.; Taunier, P.; Grand, D.; Jeantet, P.; Deleglise, M.; Roux, J. P.; Hazemann, J. L. *Phys. Scr.* **2005**, *T115*, 970.
(57) Proux, O.; Nassif, V.; Prat, A.; Ulrich, O.; Lahera, E.; Biquard, X.; Menthonnex, J. J.; Hazemann, J. L. *J. Synchrotron Radiat.* **2006**, *13*, 59.
(58) Kau, L. S.; Spira-solomon, D. J.; Penner-Hahn, J. E.; Hodgson, K. O.; Solomon, E. I. *J. Am. Chem. Soc.* **1987**, *109*, 6433.
(59) Poger, D.; Fillaux, C.; Miras, R.; Crouzy, S.; Delangle, P.; Mintz, E.; Den Auwer, C.; Ferrand, M. *J. Biol. Inorg. Chem.* **2008**, *13*, 1239.
(60) Ravel, B.; Newville, M. *J. Synchrotron Radiat.* **2005**, *12*, 537.
(61) Baumgartner, M.; Schmalle, H.; Baerlocher, C. *J. Solid State Chem.* **1993**, *107*, 63.

(62) Smith, T. A.; Lerch, K.; Hodgson, K. O. *Inorg. Chem.* **1986**, *25*, 4677.
(63) Lee, P. A.; Citrin, P. H.; Eisenberger, P.; Kincaid, B. M. *Rev. Mod. Phys.* **1981**, *53*, 769.
(64) Xiao, Z. G.; Brose, J.; Schimo, S.; Ackland, S. M.; La Fontaine, S.; Wedd, A. G. *J. Biol. Chem.* **2011**, *286*, 11047.
(65) Xiao, Z. G.; Wedd, A. G. *Nat. Prod. Rep.* **2010**, *27*, 768.
(66) Shaw, C. F.; Laib, J. E.; Savas, M. M.; Petering, D. H. *Inorg. Chem.* **1990**, *29*, 403.
(67) Vortisch, V.; Kroneck, P.; Hemmerich, P. *J. Am. Chem. Soc.* **1976**, *98*, 2821.
(68) Hefter, G.; May, P. M.; Sipos, P. *J. Chem. Soc., Chem. Commun.* **1993**, 1704.
(69) Pickering, I. J.; George, G. N.; Dameron, C. T.; Kurz, B.; Winge, D. R.; Dance, I. G. *J. Am. Chem. Soc.* **1993**, *115*, 9498.
(70) Vallee, B. L.; Auld, D. S. *Acc. Chem. Res.* **1993**, *26*, 543.

dx.doi.org/10.1021/ic5004319 | *Inorg. Chem.* 2014, 53, 5229−5239